PHYSICAL REVIEW B **69**, 140501(R) (2004)

# Antiferromagnetic domain walls in lightly doped layered cuprates

Baruch Horovitz
*Department of Physics and Ilze Katz Center for Nanotechnology, Ben-Gurion University of the Negev, Beer-Sheva 84105, Israel*
(Received 8 December 2003; published 1 April 2004)

Recent electron-spin-resonance (ESR) data show rotation of the antiferromagnetic (AF) easy axis in lightly doped layered cuprates upon lowering the temperature. We account for the ESR data and show that it has significant implications on spin and charge ordering according to the following scenario: In the high-temperature phase AF domain walls coincide with (110) twin boundaries of an orthorhombic phase. A magnetic field leads to annihilation of neighboring domain walls resulting in antiphase boundaries. The latter are spin carriers, form ferromagnetic lines and may become charged in the doped system. However, hole ordering at low temperatures favors the (100) orientation, inducing a $\pi/4$ rotation in the AF easy axis. The latter phase has twin boundaries and AF domain walls in (100) planes.

DOI: 10.1103/PhysRevB.69.140501 PACS number(s): 74.72.Bk, 75.25.+z, 75.60.Ch, 75.80.+q

The effect of holes on antiferromagnetism is a central issue in high-temperature superconductivity. In a remarkable recent experiment the role of doping in $Y_{1-x}Ca_xBa_2Cu_3O_6$ ($x \approx 0.008$) was studied by Jánossy *et al.*[1] using an electron-spin-resonance (ESR) technique. The data show that the antiferromagnetic (AF) polarization rotates from [100] at high temperatures to [110] around $\approx 40$ K. A corresponding anomaly was also seen by muon spin resonance in $Y_{1-x}Ca_xBa_2Cu_3O_6$ as well as in $La_{2-x}Sr_xCuO_4$ compounds.[2] In the undoped compound ($x=0$) the polarization remains in the [100] direction down to low temperatures.

The ESR data[1] also show that AF domains are present and that their relative intensity is controlled by magnetic fields. In the high-temperature phase with field in the [100] direction, the [010] polarized domains are preferred since the canting of AF spins has a higher susceptibility. This defines a ''depinning'' field at which the unpreferred domains are diminished. For example, at high temperatures and above a field of $\approx 1$ T 80% of the domains are polarized perpendicular to the field. The ESR data show, curiously, that the depinning field of the [110] AF of $Y_{1-x}Ca_xBa_2Cu_3O_6$ (with field in the $[1\bar{1}0]$ direction) is higher than that of the [100] AF in $YBa_2Cu_3O_6$ (field in the [010] direction), both at low temperatures.

In the present work we suggest that the transition in the AF polarization correlates with a lattice distortion and with condensation of the holes into a charge-density wave (CDW). Our reasoning involves a scenario for spin and charge ordering with the following steps.

(i) At high temperatures and weak magnetic fields the [100] polarized AF leads to an orthorhombic structure; the AF domain walls (DW's) coincide then with twin boundaries at (110) planes.

(ii) Strong magnetic fields favor one of the AF domains so that DW's annihilate. We show that this process results in antiphase boundaries (APB's) which consist of ferromagnetic lines.

(iii) At low temperatures hole ordering can occur by binding states localized at the APB's. However, hole ordering favors the (100) orientation, i.e., a CDW with maxima on (100) planes and an (incommensurate) wave vector in the [100] direction. This CDW favors an AF polarization in a diagonal [110] direction which is weakly orthorhombic with (100) twin boundaries and DW's.

An AF polarized in the [100] axis favors an orthorhombic phase since dipoles interact differently for $\rightarrow\leftarrow$ and $\uparrow\downarrow$ pairs. This magnetoelastic coupling is expected to be rather small in the cuprates, leading to a change in lattice constant of order[3] $10^{-5}$–$10^{-6}$. In principle ESR analysis can detect the resulting change in crystal field,[4] however, the effect seems too weak in the case AF $YBa_2Cu_3O_6$. Yet, this coupling can be sufficiently strong in samples of size $\approx 1$ mm so that twin boundaries are necessary to relieve macroscopic strains.

We proceed to present evidence for steps (i) and (iii), and then derive step (ii). We claim that an orthorhombic structure is in fact supported by the mere observation of AF domains. The presence of AF domains and the associated domain walls[5] are well known to result from either entropy effects (when temperature is fairly close to the Néel temperature), or from disorder or from a magnetoelastic coupling. The ESR experiment[1] has used high-purity samples and temperature was well below the Néel temperature. Hence the presence of DW's is a strong indication for the presence of the magnetoelastic coupling, supporting step (i) of the scenario above.

Step (iii) is consistent with data on the compounds[6] $La_{1.875}Ba_{0.125-x}Sr_xCuO_4$. These compounds maintain fixed carrier density while allowing for both tetragonal and orthorhombic phases. In the tetragonal phase an incommensurate CDW (as well as an incommensurate spin-density wave) with wave vector in the [100] direction is present. For systems near the orthorhombic boundary (less orthorhombic phase) the CDW wave vector deviates slightly from the [100] axis and finally the CDW disappears in the orthorhombic phase.

We propose then that the orthorhombic structure induced by the [100] polarized AF structure is unstable when holes are added and form a [100] CDW. The AF polarization then rotates to the [110] direction which, as shown below, is weakly orthorhombic and has (100) twin boundaries. We proceed now to analyze an effective free energy and study various domain walls. In particular, step (ii) is shown, i.e.,

 

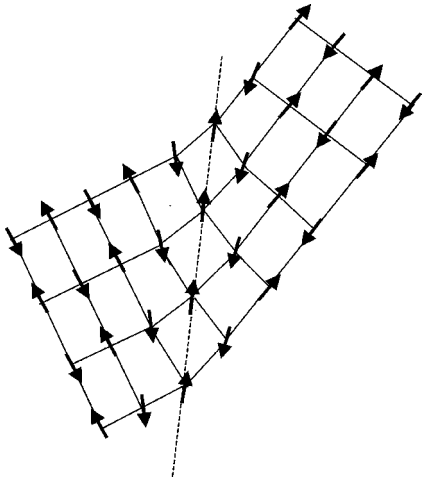

FIG. 1. Twin boundary with spin polarizations (arrows) exhibiting an AF domain wall. The dashed line is in a (110) plane and is the $s=0$ line defining a TB position. The displacement $u(s)$ is parallel to this line and yields the strain $\epsilon=\partial u/(\sqrt{2}\partial s)$ interpolating between the two orthorhombic variants.

the collapse of two neighboring magnetic DW's (e.g., by applying a magnetic field) leads to antiphase boundaries which can be detected by a variety of experiments.

Consider first the elasticity part, i.e., the tetragonal-orthorhombic (T-O) transition and formation of twin boundaries (TB's). The orthorhombic distortion, for weak strain, corresponds to a tetragonal lattice displaced in the [110] direction with a displacement $u$ that is linear in the coordinate $s$ in the $[1\bar{1}0]$ axis, i.e., $u\sim\pm s$ (see Fig. 1). The $\pm$ signs correspond to the two variants of the orthorhombic phase. The free energy, in terms of the strain $\epsilon=\partial u/(\sqrt{2}\partial s)$, has then the form[7]

$$\mathcal{F}_0=\mathcal{F}_1(\epsilon)+\frac{1}{2}c\left(\frac{\partial\epsilon}{\partial s}\right)^2, \tag{1}$$

where $\mathcal{F}_1(\epsilon)$ has a double minima corresponding to the two variants. A static solution interpolating smoothly between the two variants is then possible,[7] and is described by a function $\epsilon_{TB}(s)$. This function has necessarily an $s$ value where $\epsilon_{TB}(s)=0$ which defines a twin boundary location, hence the TB is on a (110) plane. In general, a TB orientation is uniquely determined by the type of structural transformation, i.e., smooth interpolation between variants across other planes leads to diverging elastic energies.[8] The formulation of Eq. (1) is a simple demonstration that for the T-O transition TB's are on (110) planes. A macroscopic strain which maintains the overall sample shape, e.g., by presence of a parent (tetragonal) phase,[9] imposes a TB array and determines its periodicity.

We proceed now to study the T-O transformation induced by a [100] polarized AF as well as the possible AF domain walls coexisting with TB's. An AF domain wall is defined by a localized rotation of the polarization angle $\theta$ (e.g., relative to the [100] axis) by $\pm\pi/2$, i.e., neighboring domains are polarized along [100] and [010], respectively. The coupled AF and strain structure is illustrated in Fig. 1. Note that spins perpendicular to the separating bond favor shorter bonds, therefore a TB induces a $\pi/2$ rotation in the AF polarization, as shown in the figure.

We claim that neighboring DW's have the same rotation angle $\pi/2$ (or $-\pi/2$), rather than opposite $\pi/2$ and $-\pi/2$. To show that the latter has no solution note first that the macroscopic strain which imposes the TB array does not affect the local differential equation for $\theta(s)$, instead it determines the average TB spacing[9] being an integration constant. Hence the existence of a static solution $\theta(s)$ can be deduced from dynamical stability considerations of the AF structure by itself. In particular, DW's with opposite $\pi/2$ and $-\pi/2$ rotations are unstable since by approaching each other they can annihilate and form the lower-energy ground state; in contrast, two $\pi/2$ DW's when approaching each other form a higher-energy antiphase boundary (see below), hence they are stable and a static solution is possible.

To illustrate this idea more explicitly we consider a slowly varying magnetization with a magnetoelastic coupling energy of the form $-a\epsilon\cos(2\theta)$; in particular, a [110] polarization ($\theta=\pi/4$) does not couple to this strain (the $\pi/4$ state has a weaker coupling to a different strain, as considered below). $F_1$ in Eq. (2) is replaced now by a quadratic term $+\frac{1}{2}b\epsilon^2$ since the T-O transition is driven by the magnetoelastic coupling, hence the full free energy is

$$F=-a\epsilon\cos(2\theta)+\frac{1}{2}b\epsilon^2+\frac{1}{2}c\left(\frac{\partial\epsilon}{\partial s}\right)^2+\frac{1}{2}d\left(\frac{\partial\theta}{\partial s}\right)^2, \tag{2}$$

where the constants $b,c,d$ are positive and the last term represents the spin stiffness. [A crystal field $\sim\cos(4\theta)$ from spin-orbit coupling is neglected; in fact it must be small to ensure that $\theta=0$ is a ground state.] The two orthorhombic variants correspond to $\theta=0,\pi/2$ with the strain $\epsilon=\pm a/b$.

Domain walls are solutions of the minimum condition for Eq. (2),

$$-a\cos(2\theta)+b\epsilon-c\frac{\partial^2\epsilon}{\partial^2 s}=0,$$

$$-2a\epsilon\sin(2\theta)+d\frac{\partial^2\theta}{\partial^2 s}=0. \tag{3}$$

A TB which interpolates between the variants $\epsilon=\pm a/b$ necessarily leads to rotation of the AF polarization by $\pi/2$, as in Fig. 1. We show next that a periodic TB array for which $\theta(s)$ is a monotonic function is a valid solution. Consider a segment of such a TB array where $\theta=0$ at $s=-s_0$ becomes $\theta=\pi/4$ at $s=0$ and finally rotates to $\theta=\pi/2$ at $s=s_0$; in the same interval the strain is antisymmetric, interpolating from $\epsilon$ near $a/b>0$ (assuming $a>0$) to $\epsilon$ near $-a/b<0$. Integration of Eq. (3) yields

$$\left.\frac{\partial\theta(s)}{\partial s}-\frac{\partial\theta(s)}{\partial s}\right|_{-s_0}=\frac{2a}{d}\int_{-s_0}^{s}\epsilon(s)\sin[2\theta(s)]ds. \tag{4}$$

In the interval $-s_0<s<s_0$, $\sin[2\theta(s)]>0$ is symmetric while $\epsilon$ is antisymmetric starting from positive values, hence the right-hand side of Eq. (4) is positive and approaches zero at

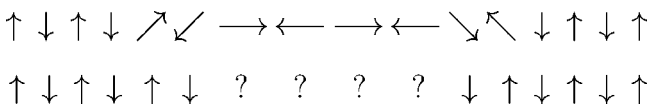

FIG. 2. The first line shows three AF variants along [100], separated by two DW's (with the diagonal polarizations). The second line shows the result of annihilation of the two DW's—the spins marked by ? continue to either left or right domains and an antiphase boundary results somewhere in the ? marked range.

$s_0$. At the next TB, $\epsilon$ is antisymmetric starting from *negative* values while $\sin[2\theta(s)]$ is symmetric and negative, hence again the right-hand side of Eq. (4) is positive. We conclude that $\partial\theta/\partial s>0$ is a consistent solution. Furthermore, in the limit $c \ll d$ the gradients are dominated by the spin stiffness while the strain follows the local AF angle, $\epsilon \approx (a/b)\cos(2\theta)$ and Eq. (3) becomes $-(a^2/b)\sin(4\theta) + d\partial^2\theta/\partial^2 s=0$. The latter is the sine-Gordon equation with well-known periodic domain structure satisfying $\partial\theta/\partial s>0$.

A $\pi/2$ DW is therefore followed by the *same* sign $+\pi/2$ DW. This result is, in fact, a robust consequence of the energy argument above requiring DW's stability, hence it is valid even with additional terms in Eq. (2). A remarkable consequence of this analysis is that when two neighboring TB's annihilate the result is not a uniform ground state, but rather a change of $\theta(s)$ by $\pi$ which is an APB, i.e., all spins on one side of the boundary are reversed relative to the ground-state orientations. The annihilation process of DW's is shown in Fig. 2. The first line shows the spin arrangement of three variants separated by two DW's with the polarization angle increasing monotonically. In the second line the DW's are eliminated, i.e., the spins are rotated so as to be aligned with either the left or the right domain. The diagonal spins join their nearest domain, but the horizontal ones can choose either domain (indicated by a ? mark), with any choice resulting in an APB somewhere in the ? marked region. Note that the APB carries an additional spin 1/2 relative to the AF ground state.

APB's involve a major rearrangement of the electronic coordinates and can result in a localized state, as shown by a mean-field study,[10] analogous to studies on solitons in polyacetylene. An APB involves therefore atomic scales and its width is of that order. In contrast, an AF DW as well as a TB have a much larger width and therefore lower formation energies. The high-energy cost of an APB, relative to that of two DW's, provides the stability of the DW array with same sign DW's.

DW's can be eliminated by a strong magnetic field as was demonstrated by the experiment of Jánossy *et al.*,[1] leading to a single variant. The process can generate APB's assuming that they are sufficiently apart and do not annihilate each other. APB's carry spin 1/2 per Cu along the boundary, i.e., a ferromagnetic line along [110] as shown in Fig. 3. These lines are AF in the [001] direction, yet, the interlayer coupling is weak so that it is relatively easy to flip magnetization by a field *parallel* to the AF polarization. Hence, when the magnetic field overcomes the interlayer coupling a nonlinear longitudinal susceptibility $\chi_\parallel$ appears due to aligned ferromagnetic lines. Note that by rotating the APB of Fig. 3 into a (100) plane its lines (within the layers) are AF rather than ferromagnetic.

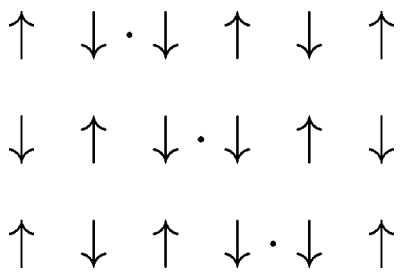

FIG. 3. An APB along a (11) line, centered on the dots, showing a ferromagnetic line. Note that the ferromagnetic polarization is parallel to that of the AF.

Consider next an alternative AF phase with polarization along [110], stabilized by terms beyond those in Eq. (2), e.g., CDW ordering (see below). The coupling of nearest neighbors along [100] or [010] is now identical and orthorhombicity is not induced, i.e., the first term in Eq. (2) vanished at $\theta=\pi/4$. However, second nearest neighbors form either $\uparrow,\uparrow$ or $\rightarrow,\rightarrow$ pairs which are nonequivalent. Hence a tetragonal unit cell which is formed by the vectors [110], $[1\bar{1}0]$, [001] of the original lattice tends to contract and expand along [110] and $[1\bar{1}0]$, respectively. This unit cell is rotated by $\pi/4$ relative to the previous one, hence the axis $s'$ along which an orthorhombic distortion alternates is now in the [100] direction, therefore twin boundaries that interpolate between $\theta=\pi/4$ and $\theta=3\pi/4$ are in (100) planes of the original tetragonal lattice. The detailed description of these TB's is more involved than the previous ones since near $\theta\approx\pi/2$ the previous strain will couple. However, following the stability argument above, we expect again a $\pi/2$ DW to be followed by the same sign $+\pi/2$ DW, hence a strong magnetic field in a [110] direction would coalesce these TB's and lead to (100) APB's.

The final ingredient in our model is that the added holes form a CDW with wave vector along [100] as clearly seen in the $La_{1.875}Ba_{0.125-x}Sr_xCuO_4$ compounds.[6] Indeed the charged APB in the mean-field calculation[10] is more strongly bound when the APB is along a (100) plane. These (100) APB's form a periodic array of stripes equivalent to a CDW with wave vector in the [010] direction. In a [100] polarized AF these (100) APB's would cross (110) DW's or (110) APB's; the [100] CDW therefore favors a rotated [110] polarized AF so that crossings with DW's are avoided. Furthermore, in a strong [110] field the [110] polarized AF has the appropriate ingredients for forming stripes, namely, (100) APB's, facilitating the CDW formation. We expect therefore that the transition temperature $T_{CDW}$ into a CDW be higher with a field in this [110] direction. The predictions for DW's and APB's are summarized in Table I as well as pertinent experimental signatures.

We show now that our model accounts also for the observation that depinning field in the [110] polarized AF $Y_{1-x}Ca_xBa_2Cu_3O_6$ is larger than that of the [100] polarized AF in $YBa_2Cu_3O_6$, both at low temperatures.[1] Depinning

TABLE I. The table lists topological structures in the AF ordering in lightly doped cuprates, as well as pertinent experimental signatures at various magnetic fields. High temperature corresponds to the [100] polarized AF phase and low temperature corresponds to the [110] polarized AF with a [100] CDW phase.

| | High temperature | Low temperature |
|---|---|---|
| Strong [100] field | (110) neutral APB ferromagnetic lines, nonlinear $\chi_{\parallel}$ | (100) DW and (100) charged APB |
| Strong [110] field | (110) DW | (100) charged APB higher $T_{CDW}$ |
| No field | (110) DW | (100) DW and (100) charged APB stronger depinning than for the undoped case |

involves annihilation of DW in pairs leading to a single domain. In $Y_{1-x}Ca_xBa_2Cu_3O_6$ some of the DW need to cross a charged APB, a process which has a barrier. In $YBa_2Cu_3O_6$ the process involves TB annihilation which is continuously achieved as field is increased with no barrier. Hence a larger depinning field in $Y_{1-x}Ca_xBa_2Cu_3O_6$.

Finally, we propose a variety of experiments for observing APB's and probing our scenario.

(i) APB's are expected to have intragap states,[10] hence optical absorption should show new lines at high magnetic fields.

(ii) The ferromagnetic nature of (110) APB lines (Fig. 3) results in a nonlinear longitudinal susceptibility $\chi_{\parallel}$.

(iii) By adding holes the APB intragap state can be charged, leading to a spinless charge carrier. These charges affect the optical absorption in (i) as well as the susceptibility in (ii).

(iv) The CDW onset is facilitated by a strong magnetic field in the [110] direction, hence $T_{CDW}$ is higher in this case.

In conclusion, our scenario accounts for the unusual ESR data[1] and predicts a variety of topological structures (Table I). We propose that experiments based on these observations can supplement the ESR data as well as clarify a central issue in high-temperature superconductivity—the nature of doping in AF layered cuprates.

## ACKNOWLEDGMENTS

I thank Professor András Jánossy for stimulating discussions and for his hospitality, and the Institute of Physics at the Budapest University of Technology and Economics for hospitality during this research. I also thank D. Golosov for pointing out Ref. 5, and A. Aharony for useful comments. This research was supported by The Israel Science Foundation founded by the Israel Academy of Sciences and Humanities.

[1] A. Jánossy, T. Fehér, and A. Erb, Phys. Rev. Lett. **91**, 177001 (2003).

[2] Ch. Niedermayer *et al.*, Phys. Rev. Lett. **80**, 3843 (1998).

[3] E. Cimpoiasu, V. Sandu, C.C. Almasan, A.P. Paulikas, and B.W. Veal, Phys. Rev. B **65**, 144505 (2002).

[4] C. Rettori *et al.*, Phys. Rev. B **47**, 8156 (1993).

[5] M.M. Farztdinov, Usp. Fiz. Nauk **84**, 611 (1964) [Sov. Phys. Usp. **7**, 855 (1965)].

[6] M. Fujita, H. Goka, K. Yamada, and M. Matsuda, Phys. Rev. Lett. **88**, 167008 (2002); Phys. Rev. B **66**, 184503 (2002).

[7] G.R. Barsch and J.A. Krumhansl, Metall. Trans. A **19A**, 761 (1988).

[8] A.G. Khachaturyan, *Theory of Structural Transformation in Solids* (Wiley, New York, 1983).

[9] B. Horovitz, G.R. Barsch, and J.A. Krumhansl, Phys. Rev. B **43**, 1021 (1991).

[10] J. Zaanen and O. Gunnarsson, Phys. Rev. B **40**, 7391 (1989); H.J. Schulz, J. Phys. (France) **50**, 2833 (1989); D. Poilblanc and T.M. Rice, Phys. Rev. B **39**, 9749 (1989); M. Kato, K. Machida, H. Nakanishi, and M. Fujita, J. Phys. Soc. Jpn. **59**, 1047 (1990).